Catalysis Communications 161 (2021) 106358

Contents lists available at ScienceDirect

Catalysis Communications

journal homepage: www.elsevier.com/locate/catcom

Short communication

# Improving the performance of Pd based catalysts for the direct synthesis of hydrogen peroxide via acid incorporation during catalyst synthesis

Richard J. Lewis [a,*], Edwin N. Ntainjua [a], David J. Morgan [a,b], Thomas E. Davies [a], Albert F. Carley [a], Simon J. Freakley [c], Graham J. Hutchings [a]

[a] Max Planck–Cardiff Centre on the Fundamentals of Heterogeneous Catalysis FUNCAT, Cardiff Catalysis Institute, School of Chemistry, Cardiff University, Main Building, Park Place, Cardiff CF10 3AT, UK
[b] Harwell XPS, Research Complex at Harwell (RCaH) Didcot, OX11 0FA, UK.
[c] Department of Chemistry, University of Bath, Claverton Down, Bath BA2 7AY, UK

ARTICLE INFO

*Keywords:*
Palladium
$H_2O_2$ direct synthesis
Green chemistry

ABSTRACT

The direct synthesis of hydrogen peroxide from molecular $H_2$ and $O_2$ offers an attractive alternative to the current means of production of this powerful oxidant, on an industrial scale. Herein we investigate the role of nitric acid addition, during catalyst preparation as a means of improving catalytic performance, under reaction conditions that have previously been found to be optimal for $H_2O_2$ production. The addition of dilute nitric acid during catalyst preparation is found to lead to a significant improvement in $H_2O_2$ synthesis activity, through the modification of particle size and control of Pd oxidation state.

## 1. Introduction

Hydrogen peroxide ($H_2O_2$) is a powerful, environmentally friendly oxidant, with the only by-product of its use being $H_2O$. Typical applications of $H_2O_2$ rely on its efficacy as a bleaching agent, such as in the paper/pulp sector or those that utilize its high active oxygen potential, for example in the synthesis of both fine and bulk chemicals [1]. The direct synthesis of $H_2O_2$ is an attractive alternative to the current means of $H_2O_2$ production on an industrial scale, the anthraquinone oxidation (AO) process, potentially allowing for the on-site production of stabilizer-free $H_2O_2$ at desirable concentrations, while also avoiding the atom efficiency concerns associated with the industrial route.

The activity of Pd based catalysts towards the direct synthesis of $H_2O_2$ has been well studied [2–4] since the first patent was grated to Henkel and Weber in 1914 [5]. However, a major challenge of catalytic selectivity has hampered the development of the direct synthesis route on an industrial scale. This can be understood as the formation of $H_2O_2$ is thermodynamically less favorable than that of $H_2O$, either directly or through the subsequent degradation of $H_2O_2$ via decomposition and hydrogenation pathways, as summarized by in Scheme 1.

Measures to improve catalytic selectivity of Pd-based catalysts towards $H_2O_2$ have typically focused on the addition of halide and acid promoters to the reaction mixture, [6–11] with the beneficial effect of these additives first reported by Pospelova et al. [12] Although, the use of such promoting agents have significant associated drawbacks, namely the need for their removal downstream, decreased reactor lifetime due to corrosion and concerns around catalyst stability. Alternatively, the addition of precious metals, such as Au [13–16] and Pt [17–19] to supported Pd catalysts have been well-reported to promote catalytic performance, often overcoming the need for acid or halide-based additives. However, from an economic perspective avoiding the use of costly secondary metals or promotive agents would be preferential.

We have previously shown that catalytic performance can be significantly enhanced through the pre-treatment of a range of supports, prior to the immobilisation of precious metal nanoparticles, through the inhibition of $H_2O_2$ degradation pathways [20–22]. However, notably this enhancement was only observed over AuPd based catalysts, with no promotion in catalytic activity observed for the analogous Pd-only catalysts. Alternatively, the use of dilute concentrations of haloacids, during catalyst synthesis has also been demonstrated to improve the performance of supported AuPd catalysts towards $H_2O_2$ production, through the enhanced formation of AuPd alloys [23,24].

With these studies in mind, we now investigate the effect of acid incorporation during the preparation of monometallic Pd catalysts on the direct synthesis of $H_2O_2$.

* Corresponding author.
*E-mail address:* LewisR27@Cardiff.ac.uk (R.J. Lewis).

https://doi.org/10.1016/j.catcom.2021.106358
Received 7 July 2021; Received in revised form 6 September 2021; Accepted 26 September 2021
Available online 27 September 2021

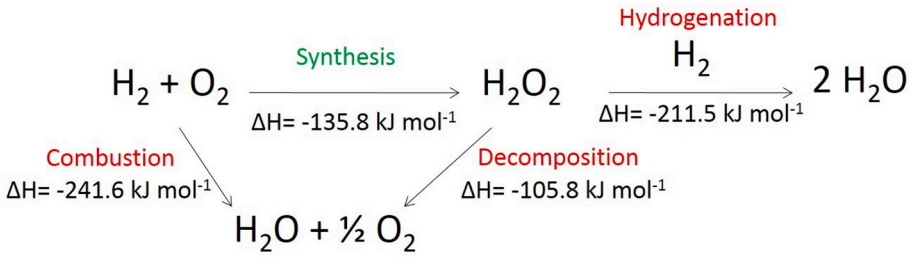


**Scheme 1.** Reaction pathways associated with the direct synthesis of $H_2O_2$ from $H_2$ and $O_2$.

## 2. Experimental

### 2.1. Catalyst preparation

**Note 1:** Catalyst preparation uses dilute $HNO_3$ and should be conducted in a ventilated fume hood.

Monometallic Pd and bimetallic AuPd (1,1 wt/wt) catalysts, with a total metal loading of 5 wt%, have been prepared on a range of supports C (G60, Merck), $TiO_2$ (P25, Evonik), $ZrO_2$ (Merck) and $CeO_2$ (Merck)) by a wet co-impregnation procedure, based on methodology previously reported in the literature, [25] in the presence and absence of $HNO_3$. The procedure to produce the 2.5%Au-2.5%Pd/C catalyst (1 g), in the presence of $HNO_3$, is outlined below, with a similar methodology used for all catalysts.

$PdCl_2$ (0.083 g, Merck), $HAuCl_4.3H_2O$ (4.082 mL, 12.25 $mgmL^{-1}$, Strem Chemicals) and $HNO_3$ (3 mL, 0.06–1.2 M, 70%, Fischer Scientific) were mixed in a 10 mL round-bottom flask and heated to 60 °C with stirring (500 rpm). Once the $PdCl_2$ was completely dissolved C (G60, 0.95 g, Merck) was added over the course of 5 min and the temperature raised to 80 °C to form a paste. The paste was dried (110 °C, 16 h) prior to calcination (flowing air, 400 °C, 3 h, 20 °C $min^{-1}$). Analogous samples were also prepared in the absence of $HNO_3$.

X-ray diffractograms of the 5%Pd catalysts, prepared in the presence and absence of $HNO_3$ [0.24 M], on a range of supports is reported in Figs. S.1–4. Total metal loading of the 5%Pd/C catalysts prepared using a range of $HNO_3$ concentrations (0.06–1.2 M, 70%) is reported in Table S.1.

### 2.2. Catalyst testing

**Note 2:** Reaction conditions used within this study operate below the flammability limits of gaseous mixtures of $H_2$ and $O_2$.

**Note 3:** The conditions used within this work for $H_2O_2$ synthesis and degradation have previously been investigated, with the presence of $CO_2$ as a diluent for reactant gases and a methanol co-solvent identified as key to maintaining high catalytic efficacy towards $H_2O_2$ production [26].

#### 2.2.1. Direct synthesis of $H_2O_2$ from $H_2$ and $O_2$

Hydrogen peroxide synthesis was evaluated using a Parr Instruments stainless steel autoclave with a nominal volume of 100 mL, equipped with a PTFE liner and a maximum working pressure of 2000 psi. To test each catalyst for $H_2O_2$ synthesis, the autoclave liner was charged with catalyst (0.01 g) and HPLC standard solvents (5.6 g methanol and 2.9 g $H_2O$). The charged autoclave was then purged three times with 5% $H_2$ / $CO_2$ (100 psi) before filling with 5% $H_2$ / $CO_2$ to a pressure of 420 psi, followed by the addition of 25% $O_2$ / $CO_2$ (160 psi). Pressure of 5% $H_2$ / $CO_2$ and 25% $O_2$ / $CO_2$ are given as gauge pressures. Reactant gas was not continually introduced into the reactor. The reaction was conducted at a temperature of 2 °C, for 0.5 h with stirring (1200 rpm), with the reactor temperature controlled using a HAAKE K50 bath/circulator using an appropriate coolant.

$H_2O_2$ productivity was determined by titrating aliquots of the final solution after reaction with acidified $Ce(SO_4)_2$ (0.0085 M) in the presence of ferroin indicator. Catalyst productivities are reported as $mol_{H_2O_2} kg_{cat}^{-1} h^{-1}$.

Total autoclave capacity was determined via water displacement to allow for accurate determination of $H_2O_2$ selectivity. When equipped with a PTFE liner, the total volume of an unfilled autoclave was determined to be 93 mL, which includes all available gaseous space within the autoclave.

Catalytic conversion of $H_2$ and selectivity towards $H_2O_2$ were determined using a Varian 3800 GC fitted with TCD and equipped with a Porapak Q column.

$H_2$ conversion (Eq. 1) and $H_2O_2$ selectivity (Eq. 2) is defined as follows:

$$H_2\text{Conversion}\ (\%) = \frac{\text{mmol}_{\text{H2 (t(0))}} - \text{mmol}_{\text{H2 (t(1))}}}{\text{mmol}_{\text{H2 (t(0))}}} \times 100 \quad (1)$$

$$H_2O_2\ \text{Selectivity}\ (\%) = \frac{H_2O_2\text{detected (mmol)}}{H_2\ \text{consumed (mmol)}} \times 100 \quad (2)$$

#### 2.2.2. Degradation of $H_2O_2$

Catalytic activity towards $H_2O_2$ degradation was determined in a similar manner to that used to measure the direct synthesis activity of a catalyst. The autoclave liner was charged with methanol (5.6 g, HPLC standard), $H_2O_2$ (50 wt%, 0.69 g), $H_2O$ (2.21 g, HPLC standard) and catalyst (0.01 g), with the solvent composition equivalent to a 4 wt% $H_2O_2$ solution. From the solution, prior to the addition of the catalyst, two 0.05 g aliquots were removed and titrated with acidified $Ce(SO_4)_2$ solution using ferroin as an indicator to determine an accurate concentration of $H_2O_2$ at the start of the reaction. The autoclave was purged three times with 5% $H_2$ / $CO_2$ (100 psi) before filling with 5% $H_2$ / $CO_2$ to a gauge pressure of 420 psi. The reaction was conducted at a temperature of 2 °C, for 0.5 h with stirring (1200 rpm). After the reaction was complete the catalyst was removed from the reaction mixture by filtration and two 0.05 g aliquots were titrated against the acidified Ce $(SO_4)_2$ solution using ferroin as an indicator. Catalytic activity towards $H_2O_2$ degradation is reported as %.

In all cases reactions were run multiple times, over multiple batches of catalyst, with the data being presented as an average of these experiments. The catalytic activity towards the direct synthesis and subsequent degradation of $H_2O_2$ was found to be consistent to within ±2% on the basis of multiple reactions.

### 2.3. Catalyst characterisation

Thermo Scientific K-Alpha$^+$ photoelectron spectrometer was used to collect XP spectra utilising a micro-focused monochromatic Al $K_\alpha$ X-ray source operating at 72 W. Samples were pressed in to a copper holder and analysed using the 400 μm spot mode at pass energies of 40 and 150 eV for high-resolution and survey spectra respectively. No charge compensation was required as the carbons were adequately conductive and gave a C(1 s) binding energy of 284.5 eV for all samples. All data was processed using CasaXPS v2.3.24 [27] using a Shirley background, Scofield sensitivity factors [28] and an electron energy dependence of

**Table 1**
Effect of $HNO_3$ (0.24 M) addition during catalyst preparation on catalytic activity towards the direct synthesis and subsequent degradation of $H_2O_2$.

| Catalyst | Productivity / $mol_{H2O2}kg_{cat}^{-1}h^{-1}$ | | $H_2O_2$ Conc. / Wt.% | | $H_2O_2$ Selectivity / % | | Degradation / % | |
|---|---|---|---|---|---|---|---|---|
| | No $HNO_3$ | $HNO_3$ added | No $HNO_3$ | $HNO_3$ added | No $HNO_3$ | $HNO_3$ added | No $HNO_3$ | $HNO_3$ added |
| 5%Pd/C | 55 | 150 | 0.11 | 0.30 | 42 | 50 | 16 | 7 |
| 5%Pd/$TiO_2$ | 24 | 89 | 0.05 | 0.18 | 21 | 52 | 16 | 23 |
| 5%Pd/$ZrO_2$ | 96 | 116 | 0.19 | 0.23 | 41 | 49 | 20 | 21 |
| 5%Pd/$CeO_2$ | 97 | 97 | 0.19 | 0.19 | 36 | 36 | 15 | 15 |

**$H_2O_2$ direct synthesis reaction conditions**: Catalyst (0.01 g), $H_2O$ (2.9 g), MeOH (5.6 g), 5% $H_2$ / $CO_2$ (420 psi), 25% $O_2$ / $CO_2$ (160 psi), 0.5 h, 2 °C 1200 rpm. **$H_2O_2$ degradation reaction conditions**: Catalyst (0.01 g), $H_2O_2$ (50 wt% 0.68 g) $H_2O$ (2.22 g), MeOH (5.6 g), 5% $H_2$ / $CO_2$ (420 psi), 0.5 h, 2 °C 1200 rpm. **n.d**: Not determined.

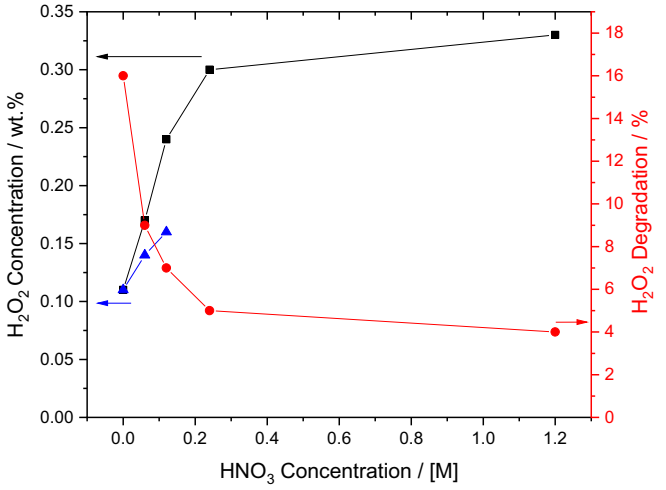


**Fig. 1.** The effect of $HNO_3$ concentration during catalyst preparation on catalytic performance of 5%Pd/carbon (G60) catalysts, towards $H_2O_2$ synthesis. **$H_2O_2$ direct synthesis reaction conditions**: Catalyst (0.01 g), $H_2O$ (2.9 g), MeOH (5.6 g), 5% $H_2$ / $CO_2$ (420 psi), 25% $O_2$ / $CO_2$ (160 psi), 0.5 h, 2 °C 1200 rpm. **$H_2O_2$ degradation reaction conditions**: Catalyst (0.01 g), $H_2O_2$ (50 wt% 0.68 g) $H_2O$ (2.22 g), MeOH (5.6 g), 5% $H_2$ / $CO_2$ (420 psi), 0.5 h, 2 °C 1200 rpm. ***Key***: Net concentration of $H_2O_2$ generated over 5%Pd/C with varying concentration of $HNO_3$ during catalyst preparation (*Black squares*). Corresponding rate of $H_2O_2$ degradation (*Red circles*). The effect of $HNO_3$ addition to the reaction solution, using 5%Pd/C catalyst prepared with no $HNO_3$ (*Blue triangles*). (For interpretation of the references to colour in this figure legend, the reader is referred to the web version of this article.)

−0.6 as recommended by the manufacturer. Peak fits were performed using a combination of Voigt-type functions and models derived from bulk reference samples where appropriate.

The bulk structure of the catalysts was determined by powder X-ray diffraction using a (θ-θ) PANalytical X'pert Pro powder diffractometer using a Cu $K_\alpha$ radiation source, operating at 40 KeV and 40 mA. Standard analysis was carried out using a 40 min run with a back filled sample, between 2θ values of 10–80°. Phase identification was carried out using the International Centre for Diffraction Data (ICDD).

Brunauer Emmett Teller (BET) surface area measurements were conducted using a Quadrasorb surface area analyser. A 5-point isotherm of each material was measured using $N_2$ as the adsorbate gas. Samples were degassed at 250 °C for 2 h prior to the surface area being determined by 5-point $N_2$ adsorption at −196 °C, and data analysed using the BET method.

Transmission electron microscopy (TEM) was performed on a JEOL JEM-2100 operating at 200 kV. Samples were prepared by dispersion in ethanol by sonication and deposited on 300 mesh copper grids coated with holey carbon film. Energy dispersive X-ray analysis (EDX) was performed using an Oxford Instruments X-Max$^N$ 80 detector and the data analysed using the Aztec software.

## 3. Results and discussion

In keeping with numerous previous works [4] our initial studies established the efficacy of monometallic Pd catalysts, prepared by a conventional wet-impregnation procedure towards the direct synthesis and subsequent degradation of $H_2O_2$ (Table 1), with all catalysts observed to be highly active towards both reaction pathways. With the exception of the $CeO_2$ supported catalyst, subsequent investigations revealed that a significant enhancement in catalytic performance can be achieved through the inclusion of $HNO_3$ (0.24 M) during catalyst preparation. Indeed, the 5%Pd/$TiO_2$ and 5%Pd/C catalysts prepared in the presence of $HNO_3$ (0.24 M) were observed to produce concentrations of $H_2O_2$ approximately three times greater than that of the analogous materials prepared in the absence of $HNO_3$. Interestingly, no similar improvement was observed for analogous AuPd catalysts (Table S.2).

With the clear enhancement in catalytic performance towards the synthesis of $H_2O_2$ we were subsequently motivated to establish the effect of $HNO_3$ concentration on catalytic performance, with a particular focus on the carbon supported materials (Fig. 1). Interestingly a significant increase in surface area is observed upon inclusion of $HNO_3$ during catalyst preparation (Table S.3). However, the observed surface area for all catalysts prepared in the presence of $HNO_3$ were found to be comparable (850–860 $m^2g^{-1}$). With numerous studies relating a similar increase in surface area after treatment with $HNO_3$ to the removal of inorganic impurities [20] and an increased functionalisation of the carbon surface [29]. It should be noted that a number of studies have determined the lack of a strong relationship between catalytic performance and surface area, with the hydrophobicity or acidity of the supports considered to be far more important [30] factors in determining catalytic efficacy. Analysis via XPS (Fig. S.5) does not reveal any significant change in oxygen concentration (increasing from ca. 10 to 12 at. % between the acid free and 1.2 M acid catalysts), which may have been expected from $HNO_3$ treatment, however given the averaging nature of XPS, then some carbon may be more oxidised than others. However, we do observe an increase in the proportion of O-functionality associated with C—O or C—OH species, as evidenced by the increase in the observed feature at 533 eV (Fig. S.5). This is concomitant with the observed increase in the feature at 286 eV in the C(1 s) spectra (Fig. S.6) which is also indicative of C—O or C—OH species.

A strong correlation was observed between the concentration of $HNO_3$ utilised in catalyst preparation and catalyst activity towards the synthesis of $H_2O_2$. Indeed, net $H_2O_2$ concentration was found to increase by a factor of three (0.33 wt%) when $HNO_3$ (1.20 M) was used in catalyst preparation, compared to the acid-free analogue (0.11 wt%), with a corresponding decrease in the rate of $H_2O_2$ degradation. We have previously demonstrated the ability of a range of materials commonly used as supports for catalysts used in the direct synthesis reaction to modify catalytic performance when used as an additive, through modification of reaction solution pH [31]. Perhaps unsurprisingly in this earlier work the addition of more basic materials, such as MgO, significantly decreased net concentrations of $H_2O_2$, whereas the addition of more

**Table 2**
Transmission Electron Microscopy (TEM) derived mean particle size and XPS determined Pd(3d5/2) FWHM for 5%Pd/C (G60) catalysts prepared with increasing $HNO_3$ concentration.

| $HNO_3$ Concentration / M | Mean particle size / nm (Standard deviation)* | FWHM for Pd(3d5/2) / eV |
|---|---|---|
| 0.0 | n.d | 1.2 |
| 0.06 | 3.4 (0.74) | 1.7 |
| 0.12 | 1.2 (0.22) | 1.7 |
| 0.24 | 2.4 (0.57) | 1.6 |
| 1.20 | 4.0 (1.00) | 1.5 |

**n.d**: unable to determine, due to lack of statistically relevant number of particles.

acidic materials led to increased $H_2O_2$ concentrations. However, in the case of carbon, the support used within this study the improvement in $H_2O_2$ concentration was negligible. With this earlier work in mind and the enhanced stability of $H_2O_2$ under acidic conditions we next determined the effect of catalyst addition on reaction solution pH (Table S.4). As with our previous study the addition of the unmodified carbon offered only a minimal decrease in reaction solution pH (6.1). However, the addition of the 5%Pd/carbon catalysts, either prepared in the presence or absence of $HNO_3$ did result in a considerable acidification of the reaction medium, although there was no correlation between the concentration of $HNO_3$ used in catalyst preparation and the measured pH, with all catalysts decreasing pH to a value of approximately 4.6. As such we do not consider that the enhanced activity of the catalysts prepared in the presence of $HNO_3$ results from a pH effect.

In keeping with our previous studies, [31] the acidification of the reaction solution with comparable concentrations of $HNO_3$ to that used in the preparation of the supported Pd catalysts did result in an improvement in the net concentration of $H_2O_2$ produced. However, the improvement in $H_2O_2$ synthesis activity was considerably lower than that observed when $HNO_3$ was used during catalyst preparation (0.16 wt % $H_2O_2$ when using an identical volume of acid to that used in the synthesis of the 5%Pd/C (0.12 M) catalyst).

The role of acid incorporation during the synthesis of AuPd catalysts has previously been demonstrated to significantly improve precious metal dispersion [23]. While studies by Tian et al. have revealed a strong correlation between catalyst performance and particle size, with sub-nano Pd species found to offer improved selectivity towards $H_2O_2$, in comparison to both larger nanoparticles or single-site analogues [32,33]. Our analysis via TEM reveals a substantial decrease in mean particle size upon the inclusion of $HNO_3$ during catalyst synthesis (Table 2, representative micrographs reported in Fig. S.7). With the acid free catalyst observed to consist of large (>100 nm) agglomerates, whereas the mean particle size of the acid-containing catalysts was found to be in the range of 1–5 nm, this change in particle size is also evidenced in XPS measurements, where there is a notable change in the FWHM of the Pd(3d) core level in the fresh catalysts [34] upon $HNO_3$ inclusion (Table 2). As with previous studies, it is therefore possible to correlate improved catalyst performance, at least partially, with an increase in nanoparticle dispersion.

The nature of Pd oxidation state has also widely been reported to be a critical factor in determining catalytic efficacy towards $H_2O_2$, with high catalytic selectivity often attributed to the presence of $Pd^{2+}$ species [35,36]. Indeed, catalysts that consist predominantly of $Pd^0$ have typically been reported to display higher rates of $H_2O_2$ degradation than $Pd^{2+}$ analogues [37]. However, there is growing consensus that the presence of mixed $Pd^{2+}$-$Pd^0$ domains is crucial in achieving high catalytic performance towards $H_2O_2$ synthesis [19,38]. This can be ascribed to the propensity of $H_2$ to dissociate on $Pd^0$ and the enhanced stability of $O_2$ on $Pd^{2+}$ surfaces, with the maintenance of the O—O bond required for the formation of $H_2O_2$. Analysis of the as-prepared 5%Pd/C catalysts prepared using a range of $HNO_3$ concentrations via XPS reveals, unsurprisingly, that after exposure to an oxidative heat treatment (400 °C, 3 h, static air) no $Pd^0$ is observed (Fig. 2.A). However, given the presence of $H_2$ in the reaction feed it is clear that the Pd oxidation state of the as-prepared materials will not be representative of those under reaction

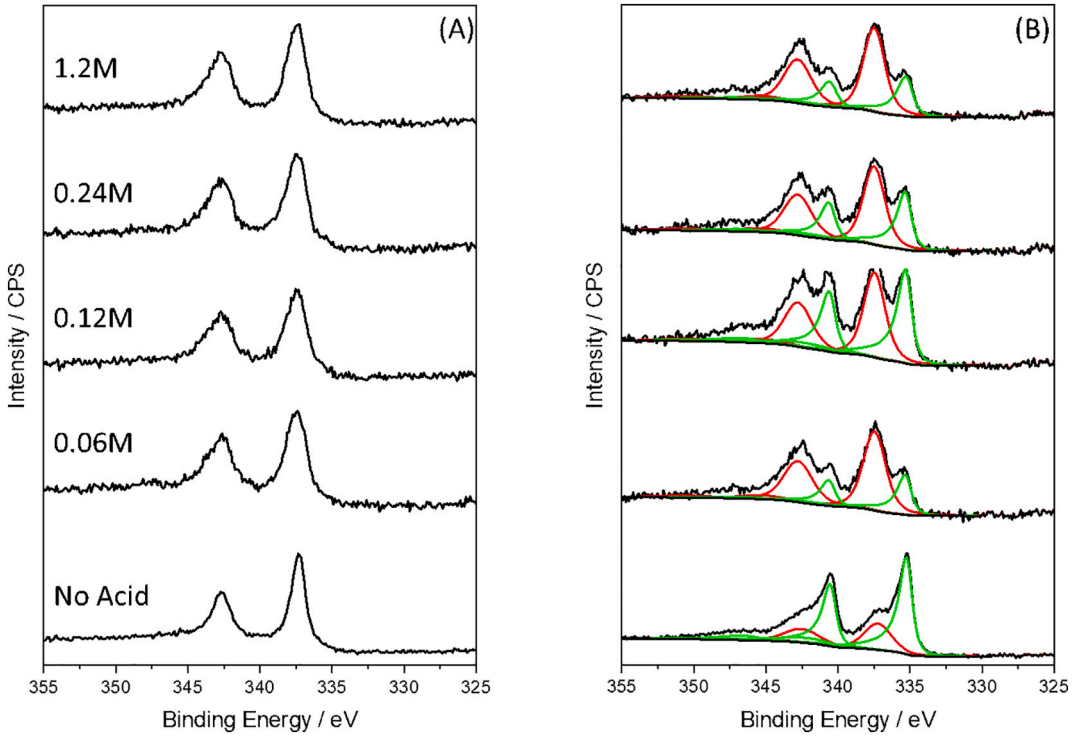


**Fig. 2.** **(A)** Fresh and **(B)** used, Pd(3d) core-level spectra illustrating the effect of $HNO_3$ concentration during catalyst preparation for 5%Pd/carbon (G60) catalysts. ***Key***: For used catalysts $Pd^0$ (*green*) and $Pd^{2+}$ (*red*). (For interpretation of the references to colour in this figure legend, the reader is referred to the web version of this article.)

conditions. Indeed, analysis of the catalysts after use in the $H_2O_2$ synthesis reaction (Fig. 2.B) reveals a shift in Pd-oxidation state, towards $Pd^0$. Interestingly, the presence of $HNO_3$ during catalyst preparation is seen to inhibit $Pd^0$ formation during the $H_2O_2$ synthesis reaction, with an apparent stabilisation of the $Pd^{2+}$ phase, which in addition to the increased nanoparticle dispersion, observed in the catalysts prepared in the presence of the acid is considered to be responsible for the enhanced performance of the catalysts prepared in the presence of $HNO_3$. The reducibility of $Pd^{2+}$ species is known to correlate well with mean particle size, with smaller nanoparticles more easily reduced than larger analogues [39]. As such it is perhaps unexpected to observe a greater proportion of $Pd^{2+}$ in the acid prepared catalysts after use in the direct synthesis reaction, as these consist of far smaller nanoparticles than the corresponding acid free catalyst. It is also important to note that our XPS analysis of the used catalysts indicate an increase of mean particle size for all catalysts as evidenced by the decrease in the FWHM of the Pd(3d) core level. Indeed, the 5%Pd/C catalyst prepared in the absence of $HNO_3$ showed the largest change in FWHM, with this value (0.9 eV) comparable to bulk Pd as measured on the same system [40]. This is perhaps understandable given the presence of very large nanoparticles (>100 nm) in the fresh materials. By comparison the FWHM of the catalysts prepared in the presence of $HNO_3$ after use in the direct synthesis reaction were also decreased, however to a far lesser extent, with the FWHM of these materials approximately (1.1 eV).

## 4. Conclusions

The incorporation of $HNO_3$ during catalyst preparation is demonstrated to significantly improve the performance of supported Pd catalysts towards $H_2O_2$ synthesis, with no comparable improvement observed in bi-metallic AuPd analogues. The ability of $HNO_3$ incorporation is found to dramatically improve control of mean nanoparticle size, as well as inhibiting the reduction of $Pd^{2+}$ species during use in the $H_2O_2$ synthesis reaction, with the presence of $Pd^{2+}$-$Pd^0$ domains known to promote catalytic selectivity towards $H_2O_2$.

## Author contributions

R.J.L, E.N.N, S.J.F and G.J.H and contributed to the design of the study; R.J.L, E.N.N and S.J.F conducted experiments and data analysis. R.J.L, E.N.N, S.J.F, D.J.M, T.E.D and A.C conducted catalyst characterisation and corresponding data processing. R.J.L, wrote the manuscript and supporting information, all authors commented on and amended both documents. All authors discussed and contributed to the work.

## Declaration of Competing Interest

There are no conflicts to declare.

## Acknowledgments

The authors wish to thank the Cardiff University electron microscope facility for the transmission electron microscopy. XPS data collection was performed at the EPSRC National Facility for XPS (‘HarwellXPS’), operated by Cardiff University and UCL, under contract No. PR16195. The Max Planck Centre for Fundamental Heterogeneous Catalysis (FUNCAT) is gratefully acknowledged for financial support.

## Appendix A. Supplementary data

Supplementary data to this article can be found online at https://doi.org/10.1016/j.catcom.2021.106358.

## References

[1] R.J. Lewis, G.J. Hutchings, Recent advances in the direct synthesis of $H_2O_2$, ChemCatChem 11 (2019) 298–308, https://doi.org/10.1002/cctc.201801435.
[2] J.S. Adams, A. Chemburkar, P. Priyadarshini, T. Ricciardulli, Y. Lu, V. Maliekkal, A. Sampath, S. Winikoff, A.M. Karim, M. Neurock, D.W. Flaherty, Solvent molecules form surface redox mediators in situ and cocatalyze $O_2$ reduction on Pd, Science 371 (2021) 626–632, https://doi.org/10.1126/science.abc1339.
[3] D.W. Flaherty, Direct synthesis of $H_2O_2$ from $H_2$ and $O_2$ on Pd catalysts: current understanding, outstanding questions, and research needs, ACS Catal. 8 (2018) 1520–1527, https://doi.org/10.1021/acscatal.7b04107.
[4] N.M. Wilson, D.W. Flaherty, Mechanism for the direct synthesis of $H_2O_2$ on Pd clusters: heterolytic reaction pathways at the liquid–solid Interface, J. Am. Chem. Soc. 138 (2016) 574–586, https://doi.org/10.1021/jacs.5b10669.
[5] H. Henkel, W. Weber (Henkel AG and Co KGaA), US1108752 A, 1914.
[6] V.R. Choudhary, C. Samanta, T.V. Choudhary, Factors influencing decomposition of $H_2O_2$ over supported Pd catalyst in aqueous medium, J. Mol. Catal. A Chem. 260 (2006) 115–120, https://doi.org/10.1016/j.molcata.2006.07.009.
[7] V.R. Choudhary, C. Samanta, P. Jana, Formation from direct oxidation of $H_2$ and destruction by decomposition/hydrogenation of $H_2O_2$ over Pd/C catalyst in aqueous medium containing different acids and halide anions, Appl. Catal., A 317 (2007) 234–243, https://doi.org/10.1016/j.apcata.2006.10.022.
[8] E. Ntainjua, M. Piccinini, J.C. Pritchard, Q. He, J.K. Edwards, A.F. Carley, J. A. Moulijn, C.J. Kiely, G.J. Hutchings, The effect of bromide pretreatment on the performance of supported au-Pd catalysts for the direct synthesis of hydrogen peroxide, ChemCatChem 1 (2009) 479–484, https://doi.org/10.1002/cctc.200900171.
[9] C. Samanta, V.R. Choudhary, Direct synthesis of $H_2O_2$ from $H_2$ and $O_2$ over Pd/H-beta catalyst in an aqueous acidic medium: influence of halide ions present in the catalyst or reaction medium on $H_2O_2$ formation, Catal. Commun. 8 (2007) 73–79, https://doi.org/10.1016/j.catcom.2006.05.027.
[10] P. Priyadarshini, T. Ricciardulli, J.S. Adams, Y.S. Yun, D.W. Flaherty, Effects of bromide adsorption on the direct synthesis of $H_2O_2$ on Pd nanoparticles: formation rates, selectivities, and apparent barriers at steady-state, J. Catal. 399 (2021) 24–40, https://doi.org/10.1016/j.jcat.2021.04.020.
[11] S.J. Freakley, R.J. Lewis, D.J. Morgan, J.K. Edwards, G.J. Hutchings, Direct synthesis of hydrogen peroxide using Au–Pd supported and ion-exchanged heteropolyacids precipitated with various metal ions, Catal. Today 248 (2015) 10–17, https://doi.org/10.1016/j.cattod.2014.01.012.
[12] T. Pospelova, N. Kobozev, Russ. J. Phys. Chem. 35 (1961) 1192–1197.
[13] J.K. Edwards, B.E. Solsona, P. Landon, A.F. Carley, A. Herzing, C.J. Kiely, G. J. Hutchings, Direct synthesis of hydrogen peroxide from $H_2$ and $O_2$ using $TiO_2$-supported Au-Pd catalysts, J. Catal. 236 (2005) 69–79, https://doi.org/10.1016/j.jcat.2005.09.015.
[14] J. Brehm, R.J. Lewis, D.J. Morgan, T.E. Davies, G.J. Hutchings, The direct synthesis of hydrogen peroxide over AuPd nanoparticles: an investigation into metal loading, Catal. Lett. (2021), https://doi.org/10.1007/s10562-021-03632-6.
[15] D. Gudarzi, W. Ratchananusorn, I. Turunen, M. Heinonen, T. Salmi, Promotional effects of Au in Pd–Au bimetallic catalysts supported on activated carbon cloth (ACC) for direct synthesis of $H_2O_2$ from $H_2$ and $O_2$, Catal. Today 248 (2015) 58–68, https://doi.org/10.1016/j.cattod.2014.04.011.
[16] J. Li, T. Ishihara, K. Yoshizawa, Theoretical revisit of the direct synthesis of $H_2O_2$ on Pd and Au@Pd surfaces: a comprehensive mechanistic study, J. Phys. Chem. C 115 (2011) 25359–25367, https://doi.org/10.1021/jp208118e.
[17] G. Bernardotto, F. Menegazzo, F. Pinna, M. Signoretto, G. Cruciani, G. Strukul, New Pd–Pt and Pd–Au catalysts for an efficient synthesis of $H_2O_2$ from $H_2$ and $O_2$ under very mild conditions, Appl. Catal., A 358 (2009) 129–135, https://doi.org/10.1016/j.apcata.2009.02.010.
[18] G. Han, X. Xiao, J. Hong, K. Lee, S. Park, J. Ahn, K. Lee, T. Yu, Tailored palladium–platinum nanoconcave cubes as high performance catalysts for the direct synthesis of hydrogen peroxide, ACS Appl. Mater. Interfaces 12 (2020) 6328–6335, https://doi.org/10.1021/acsami.9b21558.
[19] X. Gong, R.J. Lewis, S. Zhou, D.J. Morgan, T.E. Davies, X. Liu, C.J. Kiely, B. Zong, G.J. Hutchings, Enhanced catalyst selectivity in the direct synthesis of $H_2O_2$ through Pt incorporation into $TiO_2$ supported AuPd catalysts, Catal. Sci. Technol. 10 (2020) 4635–4644, https://doi.org/10.1039/D0CY01079K.
[20] J.K. Edwards, B. Solsona, E.N. Ntainjua, A.F. Carley, A.A. Herzing, C.J. Kiely, G. J. Hutchings, Switching off hydrogen peroxide hydrogenation in the direct synthesis process, Science 323 (2009) 1037–1041, https://doi.org/10.1126/science.1168980.
[21] J.K. Edwards, E.N. Ntainjua, A.F. Carley, A.A. Herzing, C.J. Kiely, G.J. Hutchings, Direct synthesis of $H_2O_2$ from $H_2$ and $O_2$ over gold, palladium, and gold–palladium catalysts supported on acid-pretreated $TiO_2$, Angew. Chem. Int. Ed. 48 (2009) 8512–8515, https://doi.org/10.1002/anie.200904115.
[22] J.K. Edwards, S.F. Parker, J. Pritchard, M. Piccinini, S.J. Freakley, Q. He, A. F. Carley, C.J. Kiely, G.J. Hutchings, Effect of acid pre-treatment on AuPd/$SiO_2$ catalysts for the direct synthesis of hydrogen peroxide, Catal. Sci. Technol 3 (2013) 812–818, https://doi.org/10.1039/C2CY20767B.
[23] M. Sankar, Q. He, M. Morad, J. Pritchard, S.J. Freakley, J.K. Edwards, S.H. Taylor, D.J. Morgan, A.F. Carley, D.W. Knight, C.J. Kiely, G.J. Hutchings, Synthesis of stable ligand-free gold–palladium nanoparticles using a simple excess anion method, ACS Nano 6 (2012) 6600–6613, https://doi.org/10.1021/nn302299e.
[24] C.M. Crombie, R.J. Lewis, R.L. Taylor, D.J. Morgan, T.E. Davies, A. Folli, D. M. Murphy, J.K. Edwards, J. Qi, H. Jiang, C.J. Kiely, X. Liu, M.S. Skjøth-Rasmussen, G.J. Hutchings, Enhanced selective oxidation of benzyl alcohol via in situ $H_2O_2$

production over supported Pd-based catalysts, ACS Catal. (2021) 2701–2714, https://doi.org/10.1021/acscatal.0c04586.
[25] E.N. Ntainjua, M. Piccinini, S.J. Freakley, J.C. Pritchard, J.K. Edwards, A.F. Carley, G.J. Hutchings, Direct synthesis of hydrogen peroxide using Au–Pd-exchanged and supported heteropolyacid catalysts at ambient temperature using water as solvent, Green Chem. 14 (2012) 170–181, https://doi.org/10.1039/C1GC15863E.
[26] A. Santos, R.J. Lewis, G. Malta, A.G.R. Howe, D.J. Morgan, E. Hampton, P. Gaskin, G.J. Hutchings, Direct synthesis of hydrogen peroxide over au–Pd supported nanoparticles under ambient conditions, Ind. Eng. Chem. Res. 58 (2019) 12623–12631, https://doi.org/10.1021/acs.iecr.9b02211.
[27] N. Fairley, V. Fernandez, M. Pichard-Plouet, C. Guillot-Deudon, J. Walton, E. Smoth, D. Flahaut, M. Greiner, M. Biesinger, S. Tougaard, D. Morgan, J. Baltrusaitis, Systematic and collaborative approach to problem solving using X-ray photoelectron spectrscopy, Appl. Surf. Sci. 5 (2021) 100112.
[28] J.H. Scofield, Hartree-slater subshell photoionization cross-sections at 1254 and 1487 eV, J. Electron Spectrosc. Relat. Phenom. 8 (1976) 129–137, https://doi.org/10.1016/0368-2048(76)80015-1.
[29] H. Hsu, C. Wang, Y. Chang, J. Hu, B. Yao, C. Lin, Graphgene oxides and carbon nanotubes embedded in polyacrylonitrile-based carbon nanofibers used as electrides for supercapacitor, J. Phys. Chem. Solids 85 (2015) 62–68, https://doi.org/10.1016/j.jpcs.2015.04.010.
[30] I. Tatsumi, H. Yuiko, N. Yohei, K. Kenji, M. Hiroshige, Pd-au bimetal supported on rutile-TiO2 for selective synthesis of hydrogen peroxide by oxidation of H2 with O2 under atmospheric pressure, Chem. Lett. 36 (2007) 878–879, https://doi.org/10.1246/cl.2007.878.
[31] R.J. Lewis, J.K. Edwards, S.J. Freakley, G.J. Hutchings, Solid acid additives as recoverable promoters for the direct synthesis of hydrogen peroxide, Ind. Eng. Chem. Res. 56 (2017) 13287–13293, https://doi.org/10.1021/acs.iecr.7b01800.
[32] P. Tian, D. Ding, Y. Sun, F. Xuan, X. Xu, J. Xu, Y.-F. Han, Theoretical study of size effects on the direct synthesis of hydrogen peroxide over palladium catalysts, J. Catal. 369 (2019) 95–104, https://doi.org/10.1016/j.jcat.2018.10.029.
[33] P. Tian, L. Ouyang, X. Xu, C. Ao, X. Xu, R. Si, X. Shen, M. Lin, J. Xu, Y.-F. Han, The origin of palladium particle size effects in the direct synthesis of H2O2: is smaller better? J. Catal. 349 (2017) 30–40, https://doi.org/10.1016/j.jcat.2016.12.004.
[34] G.K. Wertheim, S.B. DiCenzo, D.N.E. Buchanan, Noble- and transition-metal clusters: the d bands of silver and palladium, Phys. Rev. B 33 (1986) 5384–5390, https://doi.org/10.1103/PhysRevB.33.5384.
[35] G. Blanco-Brieva, E. Cano-Serrano, J.M. Campos-Martin, J.L.G. Fierro, Direct synthesis of hydrogen peroxide solution with palladium-loaded sulfonic acid polystyrene resins, ChemCommun (2004) 1184–1185, https://doi.org/10.1039/B402530J.
[36] R.J. Lewis, K. Ueura, Y. Fukuta, S.J. Freakley, L. Kang, R. Wang, Q. He, J. K. Edwards, D.J. Morgan, Y. Yamamoto, G.J. Hutchings, The direct synthesis of $H_2O_2$ using TS-1 supported catalysts, ChemCatChem 11 (2019) 1673–1680, https://doi.org/10.1002/cctc.201900100.
[37] V.R. Choudhary, S.D. Sansare, A.G. Gaikwad, Direct oxidation of $H_2$ to $H_2O_2$ and decomposition of $H_2O_2$ over oxidized and reduced Pd-containing zeolite catalysts in acidic medium, Catal. Lett. 84 (2002) 81–87, https://doi.org/10.1023/A:1021032819400.
[38] L. Ouyang, P. Tian, G. Da, X. Xu, C. Ao, T. Chen, R. Si, J. Xu, Y. Han, The origin of active sites for direct synthesis of $H_2O_2$ on Pd/$TiO_2$ catalysts: interfaces of Pd and PdO domains, J. Catal. 321 (2015) 70–80, https://doi.org/10.1016/j.jcat.2014.10.003.
[39] A. Baylet, P. Marécot, D. Duprez, P. Castellazzi, G. Groppi, P. Forzatti, In Sity Raman and in situ XRD analysis of PdO reduction and Pd0 oxidation supported on γ-Al2O3 catalyst under different atmospheres, Phys. Chem. Chem. Phys. 13 (2011) 4607–4613, https://doi.org/10.1039/C0CP01331E.
[40] G.K. Wertheim, S.B. DiCenzo, D.N.E. Buchanan, Noble- and transition-metal clusters: the d bands of silver and palladium, Phys. Rev. B 33 (1986) 5384, https://doi.org/10.1103/PhysRevB.33.5384.